Characterization of Micro-Generators Embedded in Commercial-Off-the-Shelf Watches for Wearable Energy Harvesting

Tiancheng Xue[*a], Shantnu Kakkar[a], Qianyu Lin[b] and Shad Roundy[a]
[a]University of Utah, Dept. of Mech. Eng., 1495 E 100 S, Salt Lake City, UT 84112, USA;
[b]Duke University, Durham, NC 27708, USA

ABSTRACT

This paper presents the characterization of the micro-generators embedded in Commercial-Off-The-Shelf (COTS) watches based on a generalized rotational energy harvester model which predicts the upper bound on energy generation given certain system constraints and specific inputs. We augment this generalized model to represent the actual micro-generator used in the Seiko Kinetic watch with realistic damping coefficients which allow us to identify optimizations to move the system output towards the upper bound. We have developed a mobile data logging platform which captures 6 DOF inertia data and the voltage output from the micro-generator simultaneously. We have asked 6 subjects to conduct a series of daily activities with the platform worn on different locations of the body. This effort not only serves as the experimental validation of our model but also provides insight into the state of the art in wearable kinetic energy harvesting devices that are commercially available. Finally we identify the opportunity for improvement on energy generation and show that we can increase the power by reducing the mechanical damping in the system, which might require an alternative mechanism with inherent lower friction.

Keywords: Energy harvesting, micro-generator, wearable, watch, characterization

1. INTRODUCTION

Energy harvesting provides a promising solution to powering wearable sensors 24/7 as the limited battery life is one the major obstacles to the emerging wearable technologies. The challenge of harnessing kinetic energy from the human body lies in the unpredictable nature of the low-frequency dominated human motion. Frequency up-conversion, usually achieved through plucking a piezoelectric element, is often applied in reported wearable energy harvester prototypes[1–3] to bridge the gap between the non-periodic excitation and the conventional resonant transducer. Different means to the same end, however, have already been taken in some of the COTS motion-powered quartz watches such as the Seiko Kinetic, the Swatch Autoquartz and the Citizen Eco-Drive Duo models.

Motion-powered quartz watches are a successful demonstration of energy harvesting technologies in commercial applications. These watch movements are classified as automatic quartz, which combines the advantages of an automatic watch (free from battery replacement) and a quartz watch (accuracy). Interestingly some of these watches came into the market before there was much activity in the research community on small scale energy harvesting. Yet the micro-generators embedded in these watches have not been thoroughly characterized in response to a real-world excitations with a system-level model to the authors' knowledge. Prior modeling endeavors tend to decouple the system from the real-world motion input: Wang *at el.* analyzed the magnetic generating rotor in the Seiko Kinetic in isolation with an optimization study on pole numbers[4]; Lossec *et al.* modeled the micro-generator used in Swatch Autoquartz with analysis on power capability including scaling effects[5]. In addition, the actual power output of these micro-generators under specific excitation hasn't been reported in any literature. Rough estimates such as 5 μW average from the Seiko Kinetic[2] or 600 mJ per day from the MGS26.4 fabricated by Kinetron (supplier of the micro-generators used in Swatch Autoquartz)[6] exist in prior research publications or manuals provided by the manufacturers.

In this paper we characterize the micro-generators embedded in COTS watches with a primary focus on the Seiko Kinetic. Currently all the commercially available micro-generators apply the electromagnetic induction according to Faraday's Law to convert the rotation of the eccentric weight to electricity. These watches typically implement a sophisticated speed conversion mechanism in order to directly obtain a useful voltage instead of employing a boost converter. The Seiko Kinetic uses a high ratio gear train to increase the speed while the Kinetron micro-generator applies a torsional spring as

[*] tiancheng.xue@utah.edu

Industrial and Commercial Applications of Smart Structures Technologies 2016,
edited by Steven F. Griffin, Proc. of SPIE Vol. 9801, 98010O · © 2016 SPIE
CCC code: 0277-786X/16/$18 · doi: 10.1117/12.2218993

an intermediate energy storage. In principal, all these micro-generators can be modeled as an ideal rotational energy harvester with a semicircular disk as the proof mass. This generalized model predicts the upper bound on energy generation given certain inputs while the augmented model for the actual micro-generator with specific speed conversion mechanism and other realistic constraints allows us to identify optimizations that could be made to move the system output towards the upper bound. We have developed a mobile data logging platform to capture the 6 DOF inertia data and the power output from the Seiko Kinetic watch simultaneously from real-world tests to serve as the inputs to the simulation and the experimental validation of our model respectively.

2. MODEL

2.1 Generalized rotational energy harvester model

The characterization of the micro-generators is based on a published generalized rotational harvester model[7] which predicts the upper bound on energy generation given 6 axis motion input and system constraints such as rotational inertia, eccentricity, etc. An electrical and a mechanical rotational damper are included in the model to represent extracted and lost energy respectively. This model is an analogy to the linear velocity damped resonant generator (VDRG) model[8], making the assumption that the power dissipated through an optimal viscous damper that represents the electromechanical transducer is the maximum electrical power that can be extracted from the system. All eccentric-rotor based energy harvesters including the Seiko Kinetic should in theory be limited by the predicted upper bound on power output.

The 3 dimensional model accounts for 6 axis inertial inputs. The harvester can be excited either linearly, rotationally or both. As illustrated in Figure 1, the rotation of the eccentric mass is constrained in the XY plane and the governing equations in the local XYZ coordinate are given by:

$$m\begin{bmatrix} -l\cos\phi_z\cdot\dot{\phi}_z^2 - l\sin\phi_z\cdot\ddot{\phi}_z \\ -l\sin\phi_z\cdot\dot{\phi}_z^2 - l\cos\phi_z\cdot\ddot{\phi}_z \end{bmatrix} = -m\begin{bmatrix}\ddot{X}\\ \ddot{Y}\end{bmatrix} + \begin{bmatrix}F_x\\F_y\end{bmatrix} + m\begin{bmatrix}g_x\\g_y\end{bmatrix} \tag{1}$$

$$I_G\ddot{\theta}_z = -I_G\ddot{\phi}_z - (D_e + D_m)\dot{\phi}_z + F_x l\sin\phi_z - F_y l\cos\phi_z \tag{2}$$

Where m, I_G, and l are the mass, the moment of inertia and the eccentric distance of the rotor respectively. $\ddot{X}$, $\ddot{Y}$ are the linear acceleration inputs to the system. F_x, F_y and g_x, g_y are the forces from the supporting shaft and the gravitational acceleration respectively in each local coordinate. ϕ_z denotes the relative angular displacement between the rotor and the housing, which determines the power output as:

$$P = D_e\dot{\phi}_z^2 \tag{3}$$

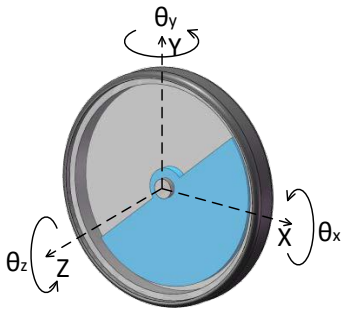

Figure 1. Dynamic model of the eccentric-rotor based rotational energy harvester

2.2 Seiko Kinetic model

The Kinetic series was first introduced by Seiko in 1986. Kinetic models with slightly different functions have come into market since its first release. The fundamental energy generation unit, however, hasn't changed much to the authors' knowledge. The only apparent improvement is that a rechargeable lithium ion battery replaced the original capacitor.

We augmented the generalized rotational energy harvester model with realistic damping coefficients to match the actual components in the 5M63, the caliber in the Seiko Kinetic watch that we analyzed in this paper. We reassembled the energy

generation unit with partial parts to identify individual mechanical loss qualitatively in each component. We applied the standard logarithmic decrement method to obtain the damping ratios quantitatively. The damping coefficients were tuned in the model to match the experimental results.

As shown in Figure 2, the energy generation unit consists of an oscillating weight, a 3-gear train, a magnetic generating rotor, a generating coil and a battery. The oscillating weight is supported by a ball bearing, which is associated with a viscous damping loss. Although Seiko claims that the rotor is suspended with magnetic levitation with no friction, by our inspection, the rotor and other gears are still supported by the standard jewel bearings used in the watch industry. Granting the fact that jewel bearings only operate well for low speed rotation, the suspension of the generating rotor is indispensable for this design to work yet hard to verify. We lump all the mechanical loss associated with the jewel bearings and gear train transmission into a coulomb damper and a viscous damper. The electromagnetic transducer is modeled as a viscous damper with respect to the generating rotor rather than the oscillating weight as in the generalized model.

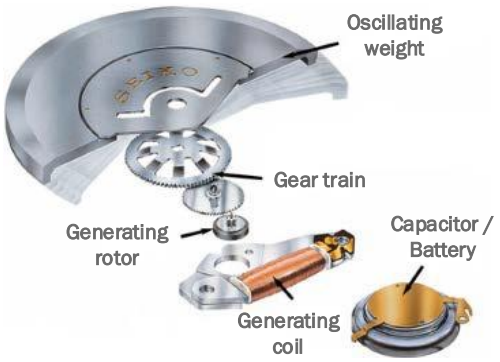

Figure 2. Exploded view of the energy generation unit in Seiko Kinetic watch[9]

Since the effective inertial torques contributed from the gears and the rotor are at least two orders of magnitude smaller than the one from the oscillating weight, we only augmented Equation (2) with the updated damping terms as follows.

$$I_G\ddot{\theta}_z = -I_G\ddot{\phi}_z - D_{m1}\dot{\phi}_z - (D_{m2} + D_e)\eta_1\eta_2\dot{\phi}_z - \mathrm{sgn}(\dot{\phi}_z)T_C + F_x l\sin\phi_z - F_y l\cos\phi_z \quad (4)$$

Where the parameters are listed in Table 1 and the power output is defined as

$$P = D_e\eta_1\eta_2\dot{\phi}_z^{\,2} \quad (5)$$

Table 1. Parameters of the Seiko Kinetic Watch model

Component	Parameter	Value
Oscillating weight	Mass m	$4.7 \times 10^{-3}\ kg$
	Moment of inertia about center of mass I_G	$2.5 \times 10^{-7}\ kg \cdot m^2$
	Moment of inertia about rotating axis I_O	$3.25 \times 10^{-7}\ kg \cdot m^2$
	Eccentricity l	$4 \times 10^{-3}\ m$
Gear train	Oscillating weight wheel to intermediate wheel ratio η_1	$1:76/7$
	Intermediate wheel to generating rotor ratio η_2	$1:61/7$
Damper	Ball bearing viscous damping coefficient D_{m1}	$1.1 \times 10^{-7}\ N \cdot m \cdot s$
	Lumped viscous damping coefficient D_{m2}	$2 \times 10^{-8}\ N \cdot m \cdot s$
	Lumped Coulomb damping torque T_C	$2.2 \times 10^{-5}\ N \cdot m$
	Electrical damping coefficient (with an optimal resistive load) D_e	$4 \times 10^{-7}\ N \cdot m \cdot s$

3. DATA COLLECTION

3.1 Mobile data logging platform

We have developed a mobile data logging platform (Gen-1) to be worn on test subjects which can capture the 6 degree of freedom inertia data and the voltage outputs from the micro-generators simultaneously. As shown in Figure 3, this Arduino based platform consists of a 9 axis BNO055 inertial measurement unit (IMU) and an Adafruit data logging shield that records inertia data as well as the voltage output of a Seiko Kinetic at 50 Hz. An RC filter was used to obtain the voltage output from the Seiko Kinetic watch. Since we removed the actual power conditioning circuit in the watch, this circuit should match the simplified electrical damper model.

A miniaturized data logger (Gen-2) based on TinyDuino platform, shown in Figure 3 as well, can sample at a higher sampling rate of 800 Hz. Note that the data presented in this paper were collected using the Gen-1 platform. We will use the Gen-2 platform for future data collection to ensure minimal hindrance to the natural motion of test subjects.

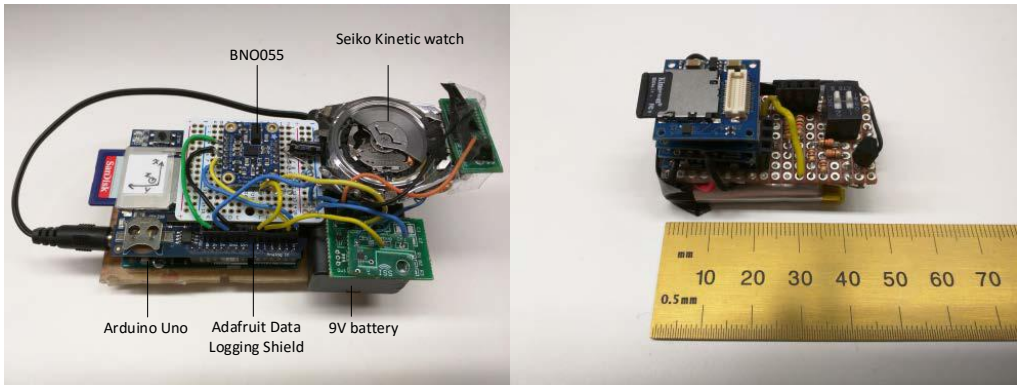

Figure 3. Photographs (not in the same scale) of the data logging platforms: Gen-1(left) and Gen-2(right).

3.2 Data collection procedure

Six subjects including both male and female participated in the data collection experiments. The data logger was attached to different body locations including the wrist, the upper arm, the chest, the waist and the upper leg using a cell phone band or bandages with Velcro. The dominant hand was chosen for attachment on the arm and the wrist. Details of the experimental set up are illustrated in Figure 4.

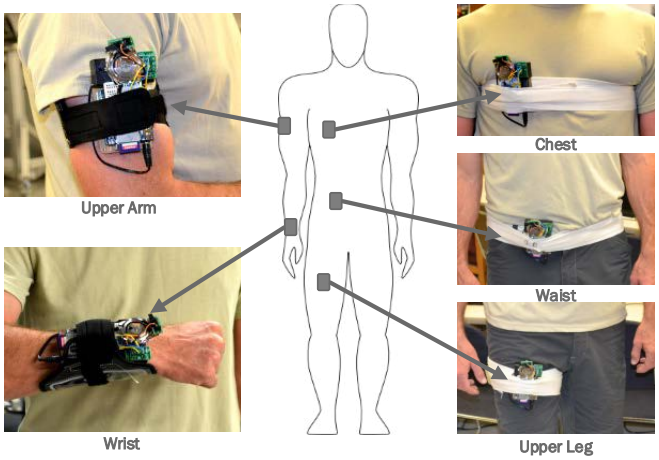

Figure 4. Photographs of the data logging platform on different body locations.

We asked all the subjects to conduct a series of daily activities including walking, jogging, running, web surfing and writing (the same text) on whiteboard. To obtain the most authentic data we specifically instructed the subjects to behave naturally and not to exaggerate the motion. Data were collected for one minute for each activity on each body location.

We have observed significant variation in activity level from subject to subject during the experiment, and thus a variation in the energy availability to harvest is expected.

4. ANALYSIS ON POWER OUTPUT

The generalized rotational harvester model provides an estimate of the maximum power output in an ideal scenario in which the electromechanical coupling can be closely approximated by an optimal linear viscous damper and mechanical damping losses (i.e. $D_m = 0$) and parasitic electrical losses are neglected. This may seem counterintuitive as assuming $D_m = 0$ in a linear vibration energy harvester would result in an optimal D_e of almost zero and infinite displacement. In our rotational case, however, there is no resonant effect as there is no restoring spring. Thus, in practice the optimal D_e is much higher than the implemented realistic D_m as observed in our simulation. Thus we take this approach to obtain the theoretical upper bound. Real-world constraints will certainly lower the actual maximum. The power output was found to be a function of the electrical damping coefficient and the eccentric rotor size. The theoretical maximum power output obtained at the optimal electrical damping coefficient at different body locations from different activities are given in Figures 5-9. The eccentric rotor applied in simulation is assumed to be made of brass with a 2mm thickness. The rotor radius ranges from 1.2 cm to 1.6 cm. Note that a small number of data are excluded in the post-processing due to an anomaly caused by an apparent motion artifact. The average power output measured from the Seiko Kinetic watch of all the subjects are marked as colored stars to match the activity with respect to its actual rotor inertia in Figures 5-9 as well. The actual power generated from web surfing and writing on whiteboard is minimal and thus not plotted.

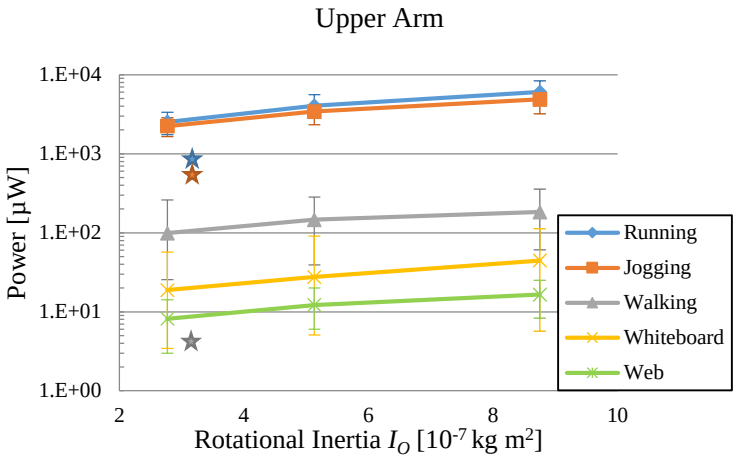

Figure 5. Average power upper bound from different activities taken at the upper arm location. The star marks the corresponding average measured power output from the Seiko Kinetic watch. The stars are color coded by activity.

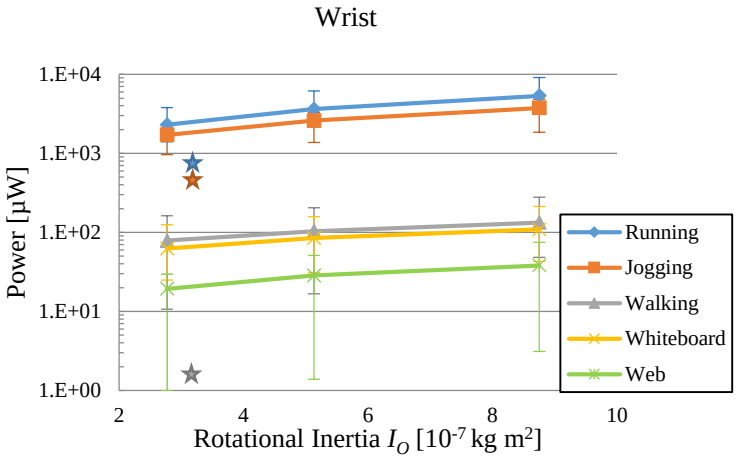

Figure 6. Average power upper bound from different activities taken at the wrist location. The star marks the corresponding average measured power output from the Seiko Kinetic watch. The stars are color coded by activity.

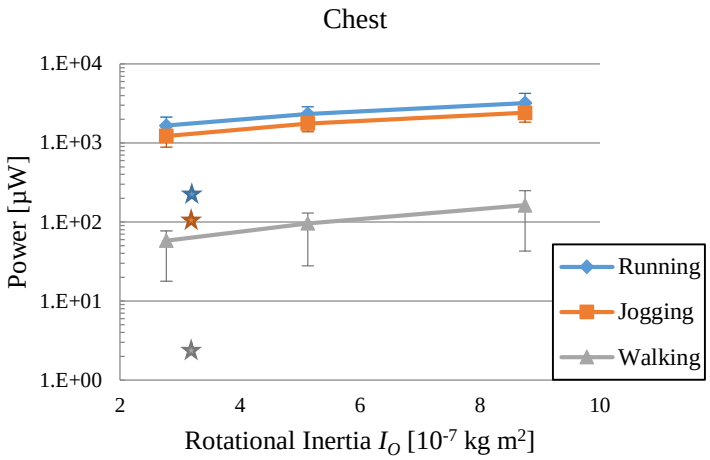

Figure 7. Average power upper bound from different activities taken at the chest location. The star marks the corresponding average measured power output from the Seiko Kinetic watch. The stars are color coded by activity.

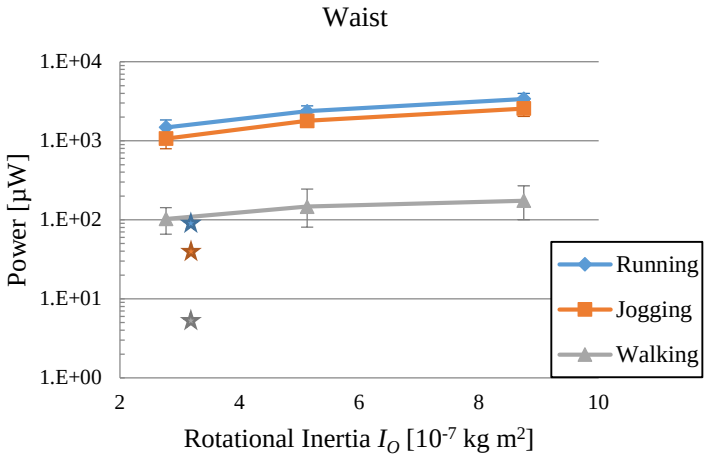

Figure 8. Average power upper bound from different activities taken at the waist location. The star marks the corresponding average measured power output from the Seiko Kinetic watch. The stars are color coded by activity.

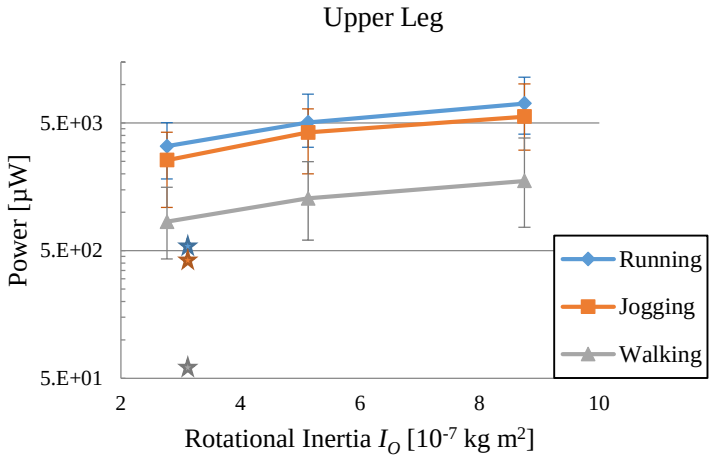

Figure 9. Average power upper bound from different activities taken at the upper leg location. The star marks the corresponding average measured power output from the Seiko Kinetic watch. The stars are color coded by activity.

As expected the power output scales with the intensity of the motion input at the same body location with running being the greatest and web surfing the least. Note that motions including web surfing and whiteboard writing involve little or no lower body motion thus the inertia data were only collected from the upper body locations. The variation in power output among different subjects, depicted as the error bar range, is in general smaller in vigorous activities such as running than in moderate activities such as walking. This agrees with the fact that the motion profile of human gait can be drastically different among the population, which is another challenge in designing a wearable energy harvester.

Additionally, these data demonstrate that a substantial gap between the theoretical maximum and what has been realized in commercial products exists. The gap among mild activities such as walking is more than one order of magnitude with the Seiko Kinetic producing less than 5 μW while the theoretical maximum is around 100 μW on the wrist. The discrepancy for more vigorous activities is smaller, but still significant. This corroborates the Coulomb damping assumption in the Seiko model, i.e. there is a static torque that the oscillating weight needs to overcome before producing power. The effect of this static torque becomes negligible when the motion is more intense.

As shown in Figure 10, the power output predicted by the Seiko Kinetic model agrees well with the measured data on an average basis given the real-world motion inputs to the nonlinear system. This system-level model allows us to identify optimizations by tuning the parameters. As a matter of fact, the power output improvement can be achieved by simply reducing the mechanical damping coefficient or the Coulomb damping torque in simulation. For example, a 24% improvement can be made by reducing the lumped damping (D_{m2} and T_C) terms by half, and a 48% improvement can be made by eliminating them in the case of the wrist location from running. In both of these cases, D_e, the electrically induced damping term, was left unchanged. If we allow the electromechanical transducer to be altered by choosing the optimal D_e, a three-time improvement can be achieved, which is close to the theoretical maximum with no friction at all. In terms of the mechanical damping itself the Coulomb damping contributes more to the mechanical loss than the viscous damping. The realization of a system with much lower mechanical damping (and an optimal level of electrically induced damping) will likely require a method of frequency up-conversion that fundamentally imposes less loss than a gear train and a high speed friction bearing.

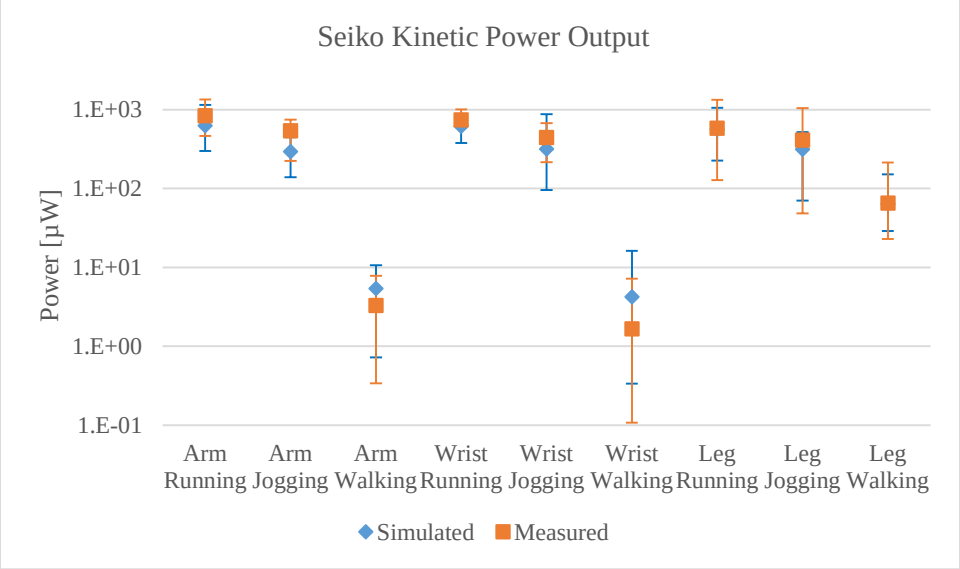

Figure 10. Average power output from the Seiko Kinetic watch: simulated vs. measured.

5. CONCLUSION

This paper has presented the characterization of the micro-generator embedded in the Seiko Kinetic watch based on a model augmented from the previously developed generalized rotational energy harvester model. We have developed a mobile data logging platform to collect power output from the Seiko Kinetic watch as well as six axis inertial data as the input to the simulation model at different body locations from multiple subjects for a series a daily activities. By comparing

the theoretical upper bound and what has been achieved through a commercial product, we have demonstrated the space for improvement on power generation. Finally we conclude that optimization could be made by tuning system parameters to increase the power output with examples of 24% to 48% improvement by reducing mechanical damping.

As an ongoing effort to collect authentic data from more represented subjects, we are upgrading the data logger platform with a higher sampling rate and a smaller form factor. We intend to apply the same modelling procedure to other COTS watch micro-generators and improve the model with the actual circuit components to allow us tune the system electrically. Most importantly we will need to experimentally realize the optimization in future work.

6. ACKNOWLEDGEMENT

This work was supported by the National Science Foundation ASSIST Nanosystems ERC under Award Number EEC-1160483.

REFERENCES

[1] Galchev, T., Kim, H.., Najafi, K., “Micro Power Generator for Harvesting Low-Frequency and Nonperiodic Vibrations,” J. Microelectromechanical Syst. **20**(4), 852–866 (2011).

[2] Pillatsch, P., Yeatman, E. M.., Holmes, A. S., “A piezoelectric frequency up-converting energy harvester with rotating proof mass for human body applications,” Sensors Actuators A Phys. **206**, 178–185 (2014).

[3] Xue, T.., Roundy, S., “Analysis of Magnetic Plucking Configurations for Frequency Up-Converting Harvesters,” J. Phys. Conf. Ser. **660**, 012098 (2015).

[4] Wang, J., Wang, W., Jewell, G. W.., Howe, D., “Design of a miniature permanent-magnet generator and energy storage system,” IEEE Trans. Ind. Electron. **52**(5), 1383–1390 (2005).

[5] Lossec, M., Multon, B.., Ahmed, H. Ben., “Micro-kinetic generator: Modeling, energy conversion optimization and design considerations,” MELECON 2010 - 2010 15th IEEE Mediterr. Electrotech. Conf., 1516–1521 (2010).

[6] Kinetron., “Micro Generator System ‘26.4,’”, <http://www.kinetron.eu/wp-content/uploads/2015/01/MGS-26.4.pdf> (21 February 2016).

[7] Xue, T., Ma, X., Rahn, C.., Roundy, S., “Analysis of Upper Bound Power Output for a Wrist-Worn Rotational Energy Harvester from Real-World Measured Inputs,” J. Phys. Conf. Ser. **557**, 012090 (2014).

[8] Mitcheson, P. D., Green, T. C., Yeatman, E. M.., Holmes, A. S., “Architectures for Vibration-Driven Micropower Generators,” J. Microelectromechanical Syst. **13**(3), 1–12 (2004).

[9] “Kinetic | Our clean energy watches | SEIKO WATCH CORPORATION.”, <http://www.seiko-cleanenergy.com/watches/kinetic-1.html> (21 February 2016).